



Ni Choine, M., Kashani, M. M., Lowes, L. N., O' Conner, A., Crewe, A. J., Alexander, N. A., & Padgett, J. E. (2016). Nonlinear dynamic analysis and seismic fragility assessment of a corrosion damaged integral bridge. *International Journal of Structural Integrity*, 7(2), 227-239. DOI: 10.1108/IJSI-09-2014-0045

Peer reviewed version

Link to published version (if available):

[10.1108/IJSI-09-2014-0045](https://doi.org/10.1108/IJSI-09-2014-0045)

[Link to publication record in Explore Bristol Research](#)

PDF-document

This is the author accepted manuscript (AAM). The final published version (version of record) is available online via Emerald at <http://www.emeraldinsight.com/doi/full/10.1108/IJSI-09-2014-0045>.

University of Bristol - Explore Bristol Research

General rights

This document is made available in accordance with publisher policies. Please cite only the published version using the reference above. Full terms of use are available: <http://www.bristol.ac.uk/pure/about/ebr-terms.html>

Nonlinear dynamic analysis and seismic fragility assessment of a corrosion damaged integral bridge

Mairéad Ni Choine¹, Mohammad M. Kashani², Laura N. Lowes³, Alan O'Connor⁴

Adam J. Crewe⁵, Nicholas A. Alexander⁶, Jamie E. Padgett⁷

Abstract

A 3D nonlinear finite element model is developed for a multi-span integral bridge with corroded reinforced concrete (RC) piers. Through a series of nonlinear dynamic time-history analyses the impact of corrosion on the seismic performance of this aging bridge is explored. To model the uncertainties associated with the material properties and corrosion models, a Monte Carlo Simulation with Latin Hypercube Sampling method is employed. A new phenomenological hysteretic model for corroded reinforcing steel is used. This model is able to simulate the combined effect of geometrical nonlinearity due to inelastic buckling of reinforcement and material nonlinearity due to yielding of material and low-cycle fatigue degradation under cyclic loading. Moreover the effect of corrosion damage on cracked cover concrete due to corrosion of vertical bars and damaged confined concrete due to corrosion of horizontal tie reinforcement are also included in the model. This study evaluates the impact of chloride induced corrosion of the RC columns on the seismic fragility of the bridge. Fragility curves are developed at a various time intervals over the lifetime. The results of this study show that the bridge fragility increases significantly with corrosion.

¹Research Engineer, Roughan & O'Donovan Consulting Engineers, Dublin, Ireland

²Lecturer, University of Bristol, Dept. of Civil Engineering University of Bristol, Bristol, BS8 1TR, United Kingdom (corresponding author), E-mail: mehdi.kashani@bristol.ac.uk

³Professor, University of Washington, Dept. of Civil and Environmental Engineering, Seattle, WA 98195-2700, United States of America

⁴Associate Professor, Trinity College Dublin, Dept. of Civil Structural & Environmental Engineering, Dublin, Ireland.

⁵Reader, University of Bristol, Dept. of Civil Engineering University of Bristol, Bristol, BS8 1TR, United Kingdom

⁶Senior Lecturer, University of Bristol, Dept. of Civil Engineering University of Bristol, Bristol, BS8 1TR, United Kingdom

⁷Associate Professor, Rice University, Dept. of Civil and Environmental Engineering, Houston, United States of America

1 Introduction

In the past couple of decades, the probabilistic assessment of highway bridges has developed rapidly in order to prioritise bridges for retrofit and rehabilitation based on their seismic risk. However, most of the current seismic risk assessment packages assume bridges remain in their as-built condition. Since many bridges which lie in earthquake prone regions have reached or passed the end of their design service life, deterioration may be an issue in many cases. Statistics in the USA show that over half of the country's bridges have reached the end of their design service life (ASCE 2013). These bridges have therefore been subject to various forms of deterioration for many years depending on their environment. Some of the main deterioration mechanisms which effect bridges are steel corrosion, concrete cracking and spalling, chemical attack, fatigue, scour and foundation settlement (FHWA 2006). Since deterioration mechanisms such as steel corrosion can have an impact on the resistance of a bridge, it is necessary to consider its effects when carrying out a seismic risk assessment.

In recent years, several researchers have carried out studies on the seismic vulnerability of corroded RC bridges. Choe et al. (2008) extended previously developed probabilistic drift and shear capacity models for pristine columns (Gardoni et al., 2002), to account for a loss of steel cross section. Using these deteriorated capacity models, seismic fragility estimates were developed for a RC corroded column in a single bent bridge. Choe et al. (2009) extended this work by developing novel probabilistic demand models for corroding RC bridges and estimated the bridge fragility by comparing the deteriorated demand models to the previously developed deteriorated capacity models. These studies found that the seismic fragility of RC columns increases over time. Simon et al. (2010) investigated the impact of concrete cover spalling and a loss of steel cross section on the seismic fragility of a RC column in a single bent bridge. This study found that a 10% loss of steel area and a loss of stiffness due to a loss of concrete cover did not have a significant effect on the seismic fragility of the selected bridge. Akiyama et al. (2011) integrated the probabilistic hazard associated with airborne chlorides into the seismic reliability of RC bridges and found that the seismic reliability of an RC bridge can be dramatically affected by the presence of airborne chlorides. This study modelled the bridge pier as a single degree of freedom (SDOF) structure and therefore, the true demands on the RC column may not have been captured. Ghosh and Padgett (2010) developed time dependant fragility curves for multi-span steel girder bridges which broadened the focus to system fragility, considering the columns, abutments and steel bearings as components in the reliability analysis. Deterioration of both the RC columns and

the steel bearings was considered and the results showed that the seismic vulnerability increases through the lifetime of the bridge. Ghosh and Padgett (2012) extended this research by developing time dependant fragility curves for aging reinforced concrete girder bridges, considering deterioration of the elastomeric bearings along with RC columns. The results of this study also showed a significant increase in seismic vulnerability with age, although it highlighted the fact that the shift in fragility strongly depends on the local environmental conditions at the bridge site and the deterioration model adopted.

For all the studies mentioned above, very simple uniaxial material models have been used to model the impact of corrosion on the stress-strain behaviour of reinforcing steel. Moreover, in most cases, the corrosion damage has been limited to the reinforcing bars (only considering an average reduced area or reduced yield strength) and the impact of corrosion on confined concrete, ductility and reduced low-cycle fatigue life is ignored. However, despite all of these simplifications, the analyses results showed that corrosion has a significant impact on the seismic fragility of corroded bridges. Moreover, recent experimental studies on the nonlinear stress-strain behaviour of corroded reinforcing bars under monotonic and cyclic loading showed that corrosion has a significant effect on hysteretic and inelastic buckling behaviour of corroded bars (Kashani et al. 2013a, b). To this end, there is a need for a more detailed and accurate numerical model to represent the impact of corrosion on reinforcing steel (including pitting effect, buckling, ductility loss and reduced low-cycle fatigue life), cracked cover concrete due to corrosion of reinforcement and reduced capacity and ductility of confined concrete due to corrosion of confinement reinforcement.

Kashani (2014) developed a detailed multi-mechanical fibre nonlinear beam-column model that includes the impact of corrosion damage on reinforcing steel (tension, buckling, reduced ductility and low-cycle fatigue), cracked cover concrete due to corrosion and reduced strength and ductility of core confined concrete due to corrosion of transverse reinforcement. This column model has been applied to a 3D bridge model, originally developed by Ni Choine et al. (2014), to investigate the impact of corrosion of the bridge piers on the nonlinear dynamic response and seismic fragility of the bridge system.

This paper firstly evaluates the impact which chloride induced corrosion of the columns has on bridge fragility. Finally, fragility curves are developed at various time intervals over the lifetime of the bridge. The results of this study show that the bridge fragility increases significantly with corrosion.

2 Proposed 3D bridge finite element model

This paper develops time dependent fragility curves for a 3-span fully integral RC bridge. The overall span length is 52m consisting of a 29m central span and two 11.5m side spans. A three-dimensional model of the bridge is developed and analysed using the OpenSees finite element platform (OpenSees 1994). Figure 1 shows the finite element model of the base bridge with modelling details of the key components highlighted. The superstructure consists of a 10m wide reinforced concrete deck slab supported on five prestressed U11 beams. The superstructure is modelled using elastic beam-column elements. There are two 6.9m columns at each bent which are modelled using nonlinear beam-column elements with fibre defined cross sections as per Kashani et al. (2014). To define the cross section, the concrete column section is discretised into fibres, made up of 16 rings and 36 wedges. The 18 reinforcing steel bars are included as an extra layer. The confined and unconfined concrete strength parameters for the columns are estimated using the approach described by Mander et al. (1989). The abutments are modelled using non-linear translational springs. Only the contribution of the piles is considered in the active direction with the pile stiffness estimated using the approach outlined by Choi (2002). In the passive direction the contribution of the soil and the piles is considered. The abutment-backfill soil interaction is modelled following the recommendations by Shamsabadi et al. (2010) whose modelling approach has been validated using experimental data on the lateral response of typical abutment systems. In the transverse direction the same passive models are adopted by altering the backbone curve to include the wing walls based on the wing wall length and participation factors. The foundations are modelled using simplified nonlinear translational and rotational springs using the method outlined by Nielson (2005). The finite element model of the bridge is updated to account for deterioration with time by reducing the steel cross sectional areas and adjusting the uniaxial material models in the columns based on the parameter estimates derived in Section 3 of this paper (Kashani et al. 2013a,b,c and Kashani 2014). The model is fully parameterised such that random variables associated with the component modelling and aging impacts can be readily incorporated in generating bridge samples for the probabilistic analysis of capacity and demand required for the time dependent fragility analysis. Uncertainties in modelling parameters are accounted for in the fragility analysis and are listed in Table 1. Further details about modelling uncertainties and probabilistic parameters are available in Ni Choine (2014).

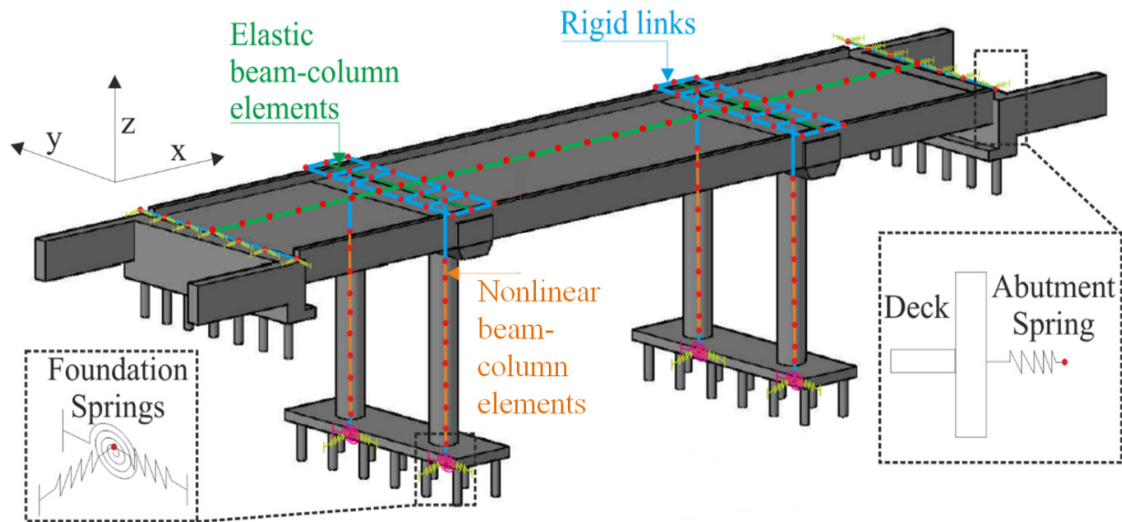


Figure 1 Three dimensional nonlinear finite element model of the 3-span integral bridge (Ní Choine, 2014)

Table 1 Statistical parameters used in finite element model of integral bridge

Parameter	Mean	Units	COV	Distribution
Steel yield strength ^a	460	MPa	0.08	Lognormal
Unconfined concrete strength ^b	30	MPa	0.08	Normal
Concrete cover depth ^c	50	mm	0.2	Lognormal
Abutment passive initial stiffness ^d	21.75	KN/mm/m	-	Uniform(14.5-28)
Pile translational stiffness ^d	7	KN/mm	-	Uniform(3.5-10.5)
Pile axial stiffness ^d	175	KN/mm	-	Uniform(87.5-262.5)
Damping ^d	0.045	ratio	0.27	Normal
Mass ^d	1.0	ratio	-	Uniform(0.9-1.1)

^aAdopted from Ellingwood & Hwang (1989)

^bAdopted from Choi (2002)

^cAdopted from Enright and Frangopol (1998)

^dAdopted from Nielson (2005)

3 Deterioration models

3.1 Chloride induced corrosion initiation and propagation

The ingress of chloride ions from the concrete surface to the level of the reinforcing steel is commonly modelled using Fick's 2nd law of diffusion as defined in Equation (1) below:

$$C(x,t) = C_s \left(1 - \operatorname{erf} \frac{x}{2\sqrt{D_c t}} \right) \quad (1)$$

where $C(x, t)$ is the chloride ion concentration at time, t , at the depth of the reinforcement, x ; C_s is the surface chloride concentration; D_c is the diffusion coefficient; and erf is the Gaussian error function. This representation of Fick's law assumes that the concentration of chlorides near the surface is relatively constant. The time to corrosion initiation, T_i , can be found when the chloride concentration at the depth of the reinforcing steel $C(x, t)$ reaches a critical level, C_{cr} , which causes dissolution of the passive film around the steel. Further detail is available in Ni Choine et al. (2014).

Once corrosion initiates, strength reduction is primarily attributed to a loss of steel cross section with time. For a reinforced concrete section with reinforcing bars of equal diameter and assuming the same initiation time for each bar, the time variant reduction in area can be found using Equation (2).

$$A(t) = \begin{cases} nD_i^2 \frac{\pi}{4} & \forall t \leq T_i \\ n(D(t))^2 \frac{\pi}{4} & \forall T_i < t < T_i + \frac{D_i}{r_{corr}} \\ 0 & \forall t \geq T_i + \frac{D_i}{r_{corr}} \end{cases} \quad (2)$$

where n is the number of reinforcement bars; D_i is the initial diameter of steel reinforcement; t is the elapsed time in years; r_{corr} is the rate of corrosion; and $D(t)$ is the reinforcement diameter at the end of years, which can be represented by Equation (3):

$$D(t) = D_i - r_{corr}(t - T_i) \quad (3)$$

In this research a constant corrosion rate was adopted from Enright and Frangopol (1998) which was identified from field data on existing bridges exposed to deicing salts. Figure 2 shows the normalised time dependent cross section loss.

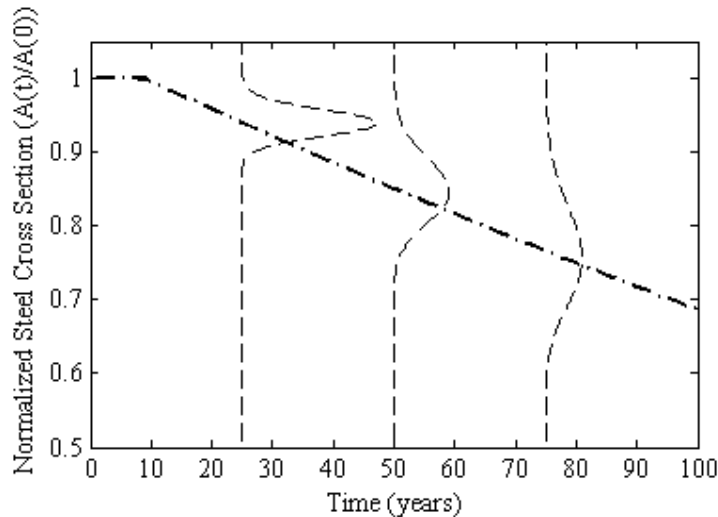


Figure 2 Distribution of normalized time variant steel cross sectional area for 40mm diameter column reinforcement

3.2 Modelling the effect of corrosion damage on reinforcing steel

In the previous section the geometrical properties of vertical reinforcement in column have been modified using the experimental data and the mathematical models available in the literature (Kashani et al. 2013a, b). The impact of corrosion pattern on nonlinear cyclic response of corroded reinforcing bars is investigated by Kashani et al. (2014) through a comprehensive nonlinear finite element analysis. Using the data generated from the nonlinear finite element analysis and experimental data (Kashani et al. 2013a, b) they have developed a new phenomenological hysteretic model for corroded reinforcing bars. The features included in the new model are including the inelastic buckling and post-buckling, reduced yield strength and ductility and low-cycle fatigue degradation due to corrosion. Once the model is validated against the experimental data of isolated corroded bars, it has been implemented in the OpenSees (Figure 3). To account for the influence of ties stiffness on cyclic behaviour of vertical reinforcement a parametric study conducted on UW-PEER (Berry et al. 2004) experimental column database. Using the parametric study data the unloading-reloading and pinching parameters of the proposed model are optimised. Further details are available in (Kashani 2014).

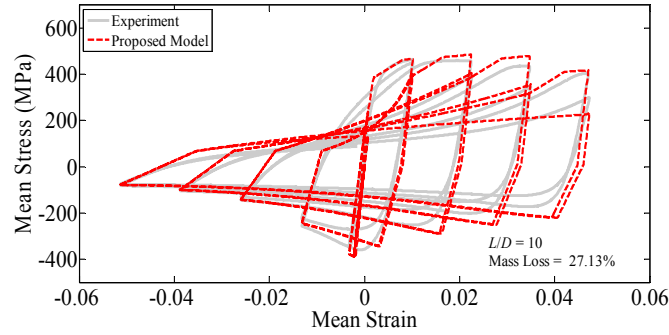
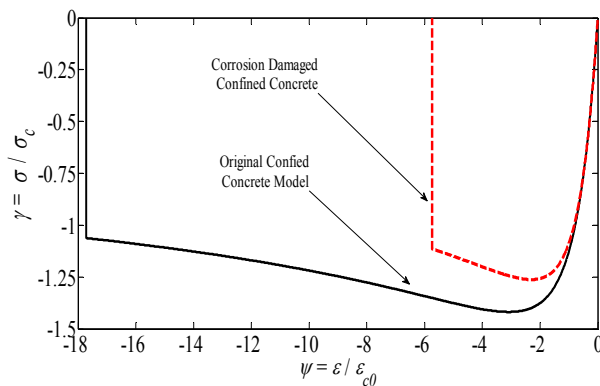


Figure 3 Example of the new phenomenological hysteretic model implemented in the OpenSees

3.3 Confined and unconfined concrete model incorporating the corrosion damage

The effect of corrosion induced cracking of cover concrete in the compression zone is considered in the analysis using the model suggested by Coronelli and Gambarova (2004). The effect of corrosion on confined concrete is considered by reducing the volumetric ratio and yield strength of confinement reinforcement as a function of steel mass loss due to corrosion. The influence of corrosion on reduced ductility is also concreted by limiting the maximum strain in confined concrete as a function of reduced ductility of hoop reinforcement (further detail is available in Kashani (2014)). The *Concrete04* available in the OpenSees is used to model both confined and unconfined concrete. The Mander's equations (Mander et al. 1988) are used to define the confinement parameters. The model suggested by Scott et al. (1982) is used to define the maximum strain in confined concrete which is associated with the fracture of first hoop reinforcement in the column. It should be noted that the unconfined concrete model is used for cover concrete and a confined concrete model is used for the core concrete. The unconfined and confined concrete models used in the analysis are shown in Figure 4.



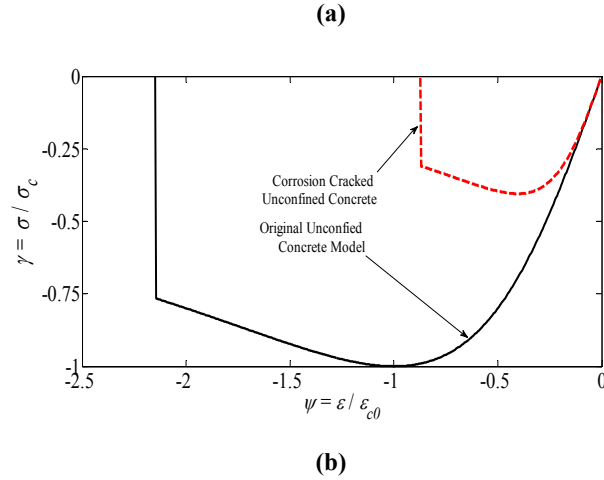


Figure 4 Material model of concrete (tension positive and compression negative): (a) confined core concrete (b) unconfined cover concrete

4 Capacity limit states

4.1 Columns

For the columns, curvature is adopted as the engineering demand parameter (EDP). Curvature limits are found through moment curvature analysis and are characterised with respect to concrete compression and steel tension strain limits taken from the literature.

In this study two limit states are defined i.e. damage control and complete collapse. The damage control state is taken as the yield curvature, ϕ_y , which is defined in Equation (4) suggested by Kwalsky (2000).

$$\phi_y = \frac{2.45 \varepsilon_y}{D_{col}} \quad (4)$$

where, ε_y is the yield strain of the longitudinal reinforcement and D_{col} is the column diameter.

The complete collapse state is taken as the curvature which corresponds to $\min\{\phi_c, \phi_{cu}, \phi_s, \phi_{su}\}$, where ϕ_{cu} is the compression strain at which fracture of the transverse confining reinforcement initiates and ϕ_{su} is the fracture strain of longitudinal steel in tension. Further detail is available in Ni Choine (2014).

4.2 Abutments

Limit states for active abutments deformations are adopted from Ramanathan (2012). Following Ramanathan (2012), the active abutment capacities are specified corresponding to the first yield and ultimate deformation of the underlying piles. In the passive and transverse directions, the limit states are taken as a function of the maximum soil displacement capacity for a given abutment height following Choi (2006). Moderate damage is defined as the maximum soil displacement capacity y_{max} , estimated as 0.05H and 0.1H for granular and cohesive soils respectively, where H is the abutment backwall height. Slight damage is taken $0.35y_{max}$. Logarithmic standard deviations of the abutment capacities are taken from Ramanathan (2012). As mentioned previously, abutments do not contribute to extensive or complete system damage.

5 Probabilistic seismic demand models

The pdfs for peak component demand to capacity ratio are predicted as a function of ground motion intensity using the peak responses from the 100 nonlinear time history analyses described above. Cornell et al. (2002) proposed that the median demand follows the power law model. However, in the proposed framework, the peak component demands of the aged bridge are divided by the capacity realisations generated using the same set of deteriorated material strength and reinforcing steel area realizations used to generate the bridge samples for a given time t . The adapted power law model is defined in Equation (5).

$$\frac{S_D(t)}{S_c(t)} = a(t) IM^{b(t)} \quad (5)$$

where, the ratio of $S_D(t)$ to $S_c(t)$ is the median demand to capacity ratio, IM is the ground motion intensity and $a(t)$ and $b(t)$ are found from regression analysis conducted in the log space. Figure 5 shows the probabilistic seismic demand to complete capacity model for the column curvature at 0 and 100 years. From the figure it can be seen that the demand experiences an increase after 100 years.

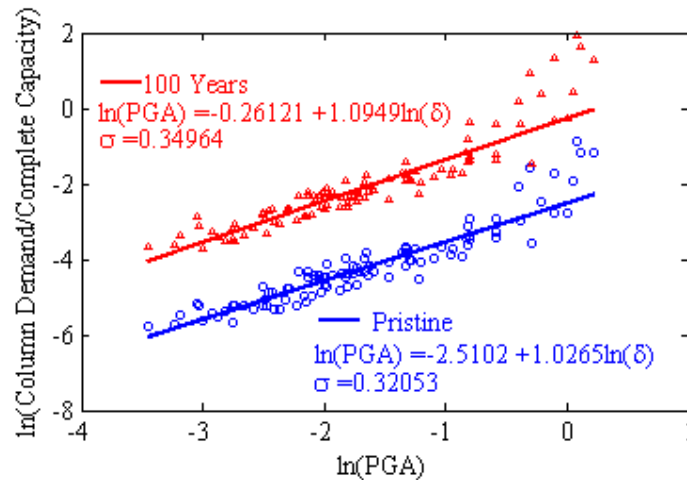


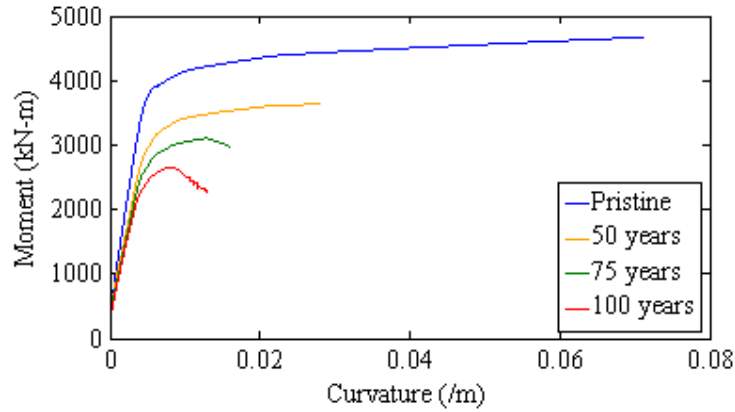
Figure 5 Probabilistic seismic demand to complete capacity model for the column curvature at 0 and 100 years

6 Impact of corrosion on response of bridge system

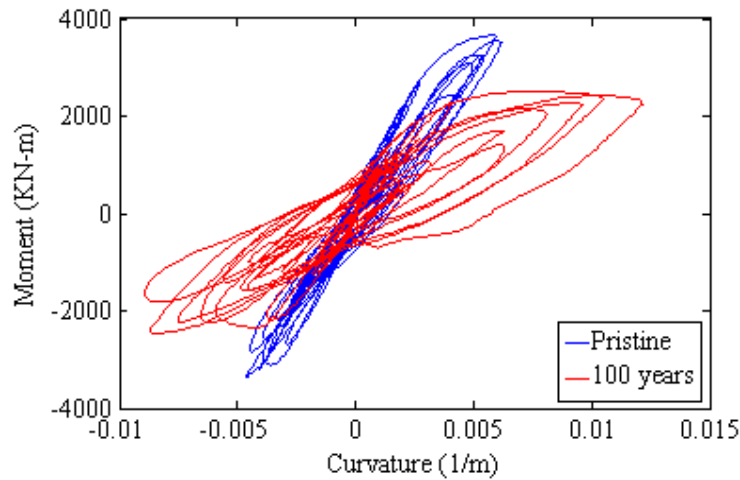
As a preliminary investigation, the OpenSees models are updated to include corrosion and the deterministic component responses are compared to the pristine responses. A time history analysis is then performed on the pristine and 100 year old base bridge subjected to the 0.99 g and 1.1 g ground motions in the longitudinal and transverse directions.

Figure 5a shows the moment curvature response at the column critical section for pristine, 50, 75 and 100 year old bridges under incremental monotonic loading and Figure 5b shows the moment curvature response at the column critical section for the pristine and 100 year old bridges under the applied ground motions in the longitudinal and transverse directions. From the figure it is clear that the maximum column curvature increases with bridge age. It is also clear that corrosion significantly affects the effective stiffness of column.

It must be noted that as well as affecting the dynamic behaviour of the bridge, corrosion and the subsequent loss of steel area and strength leads to a reduction in the load carrying capacity and yield curvature of a column.



(a)



(b)

Figure 6 Moment curvature response of column critical section: (a) incremental monotonic loading (b) time-history analysis subject to ground motions applied in the longitudinal and transverse directions simultaneously

7 Time dependent fragility analysis of the proposed bridge

A time dependent fragility analysis of the case study bridge accounting for reinforcement corrosion is first conducted to explore the effects of aging on the seismic vulnerability of integral bridges. The probabilistic analysis is conducted at four points in time along the service life of the structure to develop both component and system fragility curves thus quantifying the effects of corrosion on the seismic vulnerability of individual components as

well as the overall system. For this study, bridge fragility is evaluated at four discrete points along the service life of the structure, namely, 0, 50, 75 and 100 years.

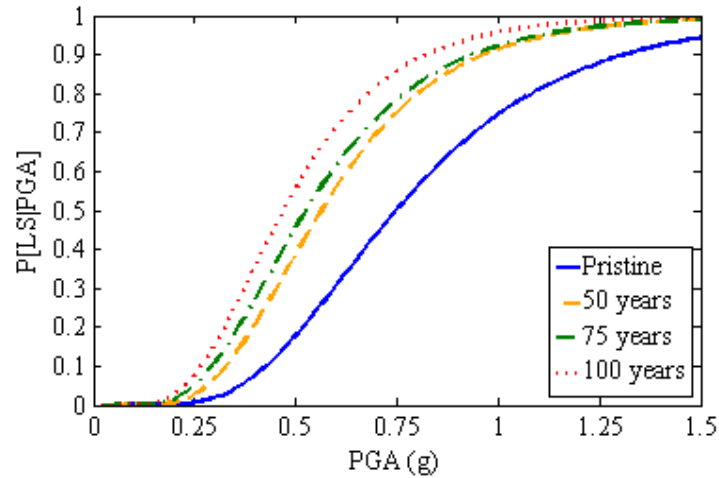
Lognormal distributions are assumed for the bridge component demand and capacity models, consistent with the literature (Nowak 1994, Ramanathan 2012), and therefore a closed-form solution for the component fragility can be found (Melchers 1999). The time dependent component fragility or conditional probability of the aged bridge demand to capacity ratio exceeding 1.0 for a given intensity is defined by Equation (6).

$$P\left(\frac{\text{Demant}(t)}{\text{Capacity}(t)} > 1.0 | IM\right) = \Phi\left(\frac{\ln\left(\frac{S_D(t)}{S_c(t)}\right)}{\sqrt{\beta^2_{D|IM}(t) + \beta^2_c(t)}}\right) \quad (6)$$

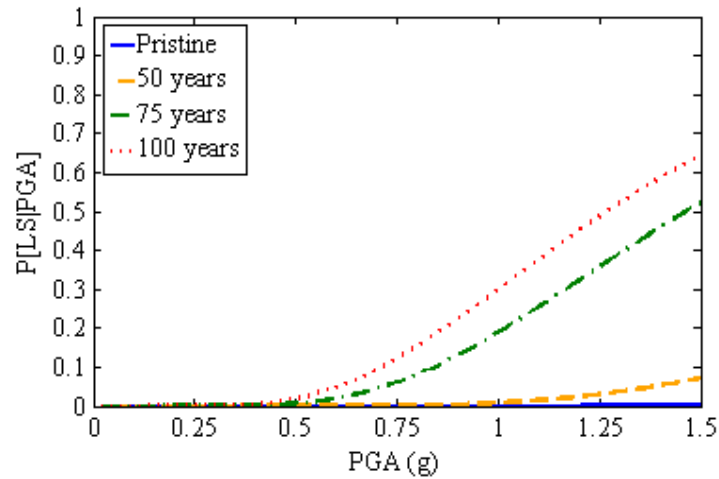
where, where $S_D(t)$ and $\square_{D|IM}(t)$ are the median and dispersion of the lognormally distributed seismic demand and $S_c(t)$ and $\square_c(t)$ are the median and dispersion of the lognormally distributed component capacity.

From the results of the component fragility analysis, it is noted that the columns experience an increase in vulnerability with age. For example, the probability of exceeding the column damage control state for the 10% in 50 year earthquake increases from 17.8% to 55.8% after 100 years.

The system fragility curves are shown in Figure 6. At the damage control state, depending on the level of deterioration, it is found that the columns and the abutments contribute to the system fragility. At the life control damage state however, it is found that the columns tend to dominate the bridge system fragility, regardless of the level of deterioration. At the life control limit state, for the 2% in 50 year earthquake, it is found that there is 30% increase in fragility after 100 years. In order to highlight the effect of the improved RC column model, these results are compared to a study that carried out a time dependent fragility analysis on the same bridge, using a simplified deterioration model only accounting for a loss of steel cross section and ductility (Ní Choine, 2014). At the life control limit state, for the 2% in 50 year earthquake, this study showed only a 3% increase in fragility after 50 years.



(a)



(b)

Figure 7 Time-variant column fragility curves

8 Conclusions

A methodology for time dependent fragility analysis is presented in this paper, such that the consideration of aging on bridge capacity and seismic demands are jointly incorporated when assessing the probabilistic seismic performance of bridge components and systems. The approach is applied for a multi-span concrete integral bridge to test the significance of accounting for both corrosion and pier settlement on this popular bridge type. The main conclusions of this study are summarised as follows:

- 1) It was found that columns dominate the system fragility at all levels of deterioration. Therefore, it highlights the importance of good column design in terms of both seismic detailing and durability for this integral bridge type.
- 2) The results of the fragility analysis also show that this type of integral bridge performs well overall under seismic loads, which is consistent with the general trend of adopting jointless bridges in high seismic zones.
- 3) It was found that corrosion has a significant effect on bending moment capacity, curvature ductility and effective stiffness of the columns.
- 4) Ageing considerations are currently neglected in widespread regional risk assessment and loss estimation packages for transport infrastructure. The result of this study provides a methodology that enables bridge managers and owners to employ in seismic risk assessment of existing aging bridges.
- 5) Additional deterioration mechanisms such as a loss of bond strength between the steel and the concrete may need to be investigated, along with the incorporation of foundation vulnerability in the fragility analysis in the future research.

References

- ASCE. *Report card for America's infrastructure*. 2013 [cited 2013 May 27th]; Available from: <http://www.infrastructurereportcard.org/a/#p/bridges/overview>.
- FHWA. 2006. Development of a Comprehensive Plan for a Long-Term Bridge Performance Program. Report No:DTFH61-05-RA-00105. Federal Highway Administration.
- Akiyama, M., Frangopol, D. M. & Matsuzaki, H. 2011. Life-cycle reliability of RC bridge piers under seismic and airborne chloride hazards. *Earthquake Engineering and Structural Dynamics*, 40, 1671-1687.
- Berry, M., Parrish, M., Eberhard, M. 2004. Performance Database User's Manual. PEER, *Univ. of Calif. Berkeley*, www.ce.washington.edu/~peera1.
- Berto, L., Vitaliani, R., Saetta, A. & Simioni, P. 2009. Seismic assessment of existing RC structures affected by degradation phenomena. *Structural Safety* 31: 284–297.

Biondini, F., Camnasio, E. & Palermo, A. 2013. Lifetime seismic performance of concrete bridges exposed to corrosion. *Structure and Infrastructure Engineering*; DOI: 10.1080/15732479.2012.761248.

Choe, D., Gardoni, P., Rosowsky, D. & Haukaas, T. 2008. Probabilistic capacity models and seismic fragility estimates for RC columns subject to corrosion. *Reliability Engineering and System Safety* 93: 383–393.

Choe, D.E., Gardoni, P., Rosowsky, D. & Haukaas, T. 2009. Seismic fragility estimates for reinforced concrete bridges subject to corrosion. *Structural Safety*, 31, 275-283.

Choi, E. 2002 Seismic analysis and retrofit of Mid-America bridges. PhD Thesis, Georgia Institute of Technology.

Cornell, C.A., Jalayer, F., Hamburger, R.O. & Foutch, D.A. 2002. Probabilistic basis for 2000 SAC federal emergency management agency steel moment frame guidelines. *Journal of Structural Engineering*, 4: 526-533.

Coronelli, D. & Gambarova P. 2004. Structural assessment of corroded reinforced concrete beams: Modeling guidelines. *Journal of Structural Engineering*; 130 (8): 1214-1224.

Ellingwood, B. & Hwang, H. 1985. Probabilistic descriptions of resistance of safety-related structures in nuclear plants. *Nuclear Engineering and Design*, 2: 169-78

Enright, M.P. & Frangopol, D.M. 1998. Probabilistic analysis of resistance degradation of reinforced concrete bridge beams under corrosion. *Engineering Structures*, 11: 960-971.

FHWA. 2006. Development of a comprehensive plan for a long-term bridge performance program. Report No: DTFH61-05-RA-00105. Federal Highway Administration, Washington, DC.

Gardoni, P., Der Kiureghian, A. & Mosalam, K. 2002. Probabilistic capacity models and fragility estimates for reinforced concrete columns based on experimental observations. *Journal of Engineering Mechanics*, 128, 1024-1038.

Ghosh, J. & Padgett, J.E. 2010. Aging considerations in the development of time-dependent seismic fragility curves. *Journal Structural Engineering*, 136 (12): 1497–1511.

Ghosh, J. & Padgett, J. E. 2012. Impact of multiple component deterioration and exposure conditions on seismic vulnerability of concrete bridges. *Earthquake and Structures*, 3, 649-673.

Kashani, M.M., Crewe, A.J., & Alexander, N.A. 2013a. Nonlinear stress-strain behaviour of corrosion-damaged reinforcing bars including inelastic buckling; *Engineering Structures*, 48: 417–429.

Kashani, M.M., Crewe, A.J., & Alexander, N.A. 2013b. Nonlinear cyclic response of corrosion-damaged reinforcing bars with the effect of buckling. *Construction and Building Materials*, 41: 388-400.

Kashani, M.M., Crewe, A.J., & Alexander, N.A. 2013c. Use of a 3D optical measurement technique for stochastic corrosion pattern analysis of reinforcing bars subjected to accelerated corrosion. *Corrosion Science*, 73: 208-221.

Kashani, M.M. 2014 Seismic Performance of Corroded RC Bridge Piers: Development of a Multi-Mechanical Nonlinear Fibre Beam-Column Model, PhD Thesis, University of Bristol.

Kashani, M.M., Lowes, L.N, Crewe, A.J. & Alexander NA. 2014. Finite element investigation of the influence of corrosion pattern on inelastic buckling and cyclic response of corroded reinforcing bars *Engineering Structures* 75: 113–125.

Kowalsky, M., 2000. Deformation Limit States for Circular Reinforced Concrete Bridge Columns. *Journal of Structural Engineering*, 8: 869-878.

Mander J.B., Priestley, M.J.N. & Park R. 1998. Theoretical stress-strain model for confined concrete. *Journal of Structural Engineering*, 114 (8): 1804-1825.

Ni Choine, M. 2014. Seismic reliability assessment of aging integral bridges, PhD Thesis, Trinity College Dublin.

Nielson, B.G. 2005 *Analytical fragility curves for highway bridges in moderate seismic zones* Ph.D., Georgia Institute of Technology.

Open System for Earthquake Engineering Simulation (OpenSees), Version 2.0.0. 2010, *Pacific Earthquake Engineering Research Centre (PEER)*.

Ramanathan, K.N. 2012 *Next generation seismic fragility curves for California bridges incorporating the evolution in seismic design philosophy* PhD Thesis, Georgia Institute of Technology.

Shamsabadi, A., P. Khalili-Tehrani, Stewart, J.P. & Taciroglu. E. 2010. Validated simulation models for lateral response of bridge abutments with typical backfills. *Journal of Bridge Engineering*, 3: 302-311.

Simon, J., Bracci, J. M. & Gardoni, P. 2010. Seismic response and fragility of deteriorated reinforced concrete bridges. *Journal of Structural Engineering*, 136, 1273-1281.

Accepted Manuscript